PNAS RESEARCH ARTICLE | BIOCHEMISTRY

USP16 is an ISG15 cross-reactive deubiquitinase that targets pro-ISG15 and ISGylated proteins involved in metabolism

Jin Gan[a,b], Adán Pinto-Fernández[c,d], Dennis Flierman[a], Jimmy J. L. L. Akkermans[e], Darragh P. O'Brien[d], Helene Greenwood[d], Hannah Claire Scott[c], Günter Fritz[f], Klaus-Peter Knobeloch[g,h], Jacques Neefjes[e], Hans van Dam[a], Huib Ovaa[a,1], Hidde L. Ploegh[b,2], Benedikt M. Kessler[c,d], Paul P. Geurink[a,2], and Aysegul Sapmaz[a,2]

Contributed by Hidde L. Ploegh; received September 12, 2023; accepted November 2, 2023; reviewed by Vishva Dixit and Alexander Varshavsky

Interferon-induced ubiquitin (Ub)-like modifier ISG15 covalently modifies host and viral proteins to restrict viral infections. Its function is counteracted by the canonical deISGylase USP18 or Ub-specific protease 18. Notwithstanding indications for the existence of other ISG15 cross-reactive proteases, these remain to be identified. Here, we identify deubiquitinase USP16 as an ISG15 cross-reactive protease by means of ISG15 activity-based profiling. Recombinant USP16 cleaved pro-ISG15 and ISG15 isopeptide-linked model substrates in vitro, as well as ISGylated substrates from cell lysates. Moreover, interferon-induced stimulation of ISGylation was increased by depletion of USP16. The USP16-dependent ISG15 interactome indicated that the deISGylating function of USP16 may regulate metabolic pathways. Targeted enzymes include malate dehydrogenase, cytoplasmic superoxide dismutase 1, fructose-bisphosphate aldolase A, and cytoplasmic glutamic-oxaloacetic transaminase 1. USP16 may thus contribute to the regulation of a subset of metabolism-related proteins during type-I interferon responses.

ISG15 | activity-based probe | USP16 | ISGylation | metabolism

Significance

Among the strongest interferon-induced proteins is ISG15, which structurally resembles a head-to-tail dimer of ubiquitin (Ub). ISG15-specific E1-, E2-, and E3-type activities catalyze ISGylation of host proteins. This requires a prior proteolytic conversion of pro-ISG15 to its mature form by USP18. USP18 is also capable of deISGylation. Application of activity-based protein profiling shows that the deubiquitinase USP16 can likewise convert pro-ISG15 to mature ISG15, as well as deISGylate host substrates. Prominent substrates for USP16-mediated deISGylation include enzymes involved in metabolism, suggesting a possible role for the ISGylation cycle in the control of metabolism in response to interferons. Multiple DUBs thus control the levels of ISGylation upon exposure to interferons, as would occur during virus infection or inflammation.

The innate immune system serves as a first line of defense against viral and bacterial infections. Its activation initiates the release of type-I interferons (mainly IFN-α and IFN-β), which induces transcription of more than 300 interferon-stimulated genes (ISGs). These ISGs encode different proteins, such as cytokines, chemokines, transcription factors, as well as enzymes that regulate the host immune response. One of the most strongly induced proteins is ISG15 (ISG of ~15 kDa), a ubiquitin (Ub)-like modifier. The structure of ISG15 resembles that of a linear Ub dimer (1, 2).

ISG15 is translated as a 17.8-kDa precursor protein, which is then processed to mature ISG15 by exposure of its carboxy-terminal Leu-Arg-Leu-Arg-Gly-Gly motif (3). This conversion is essential to enable the covalent modification of substrate proteins with ISG15. Mature ISG15 can be secreted from cells and act as a cytokine (4–7). Upon interaction of ISG15 with intracellular target proteins it can modulate their functions (8, 9) and stability (10). ISG15 can also be conjugated covalently to ε-amines of target proteins via the ISG15 conjugation cycle (ISGylation), a process analogous to ubiquitination. ISG15 conjugation is mediated by a sequential E1-E2-E3 enzyme cascade, which includes an E1, UBE1L (UBA7) (11), an E2, UBE2L6 (12, 13), and the E3s HERC5 (14), TRIM25 (15), and HHARI (16) in human cells and mHERC6 (17, 18) in murine cells. ISGylation of proteins regulates their turnover (19–21) and influences complex formation (22, 23).

ISG15 is deconjugated by specific proteases in a process termed deISGylation, analogous to Ub removal by deubiquitinases (DUBs). The major deISGylating enzyme identified in mammalian cells is USP18 (24), a member of the Ub-specific protease (USP) family, but USP18 does not remove Ub from ubiquitinated proteins. The substrate specificity, structure, and the role of USP18 in innate immunity have been well-characterized (25–28). While USP18 processes pro-ISG15, ablation of USP18 protease activity in vivo does not impair the ISGylation machinery (28), indicating that other proteases with deISGylase activity must exist. Since Ub and ISG15 share a common protein fold and an identical C-terminal tail (Leu-Arg-Leu-Arg-Gly-Gly), other members from the Ub-specific peptidase (USP) family, similar to USP18, may be able to process pro-ISG15 into its mature form. Indeed, in vitro experiments showed covalent interactions of USP2, USP5, USP13, USP14, and USP21 with ISG15-based probes (29–31). The deISGylase activity of USP5, USP14, and USP21 was confirmed in vitro (29, 32). However, whether the ISG15 cross-reactivity of these DUBs extends to living cells remains to be determined. Because pro-ISG15 processing continues in the absence of USP18 activity, we explored ISG15-cross-reactive DUBs and addressed the possible biological relevance of their deISGylase activity.

Reviewers: V.D., Genentech; and A.V., California Institute of Technology.

The authors declare no competing interest.

[1]Deceased May 19, 2020.

[2]To whom correspondence may be addressed. Email: hidde.ploegh@childrens.harvard.edu, p.p.geurink@lumc.nl, or a.sapmaz@lumc.nl.

This article contains supporting information online at https://www.pnas.org/lookup/suppl/doi:10.1073/pnas.2315163120/-/DCSupplemental.

Published December 6, 2023.

To identify deISGylating enzymes in an unbiased manner, we used ISG15 activity-based protein profiling (ABPP) assays to detect deISGylating enzymes in human HAP1 cell lysates. USP18, USP5, and USP14 were identified as deISGylating enzymes in this assay, corroborating previous studies. We identified USP16, a DUB that regulates the ubiquitination of H2A (33), RPS27a (34), and IKKβ (35), as an ISG15-cross-reactive DUB. USP16 cleaved both pro-ISG15 and isopeptide-linked ISG15-based fluorescence polarization (FP) substrates in vitro, as well as endogenous ISGylated substrates in a cell lysate.

In order to identify ISGylated substrates of USP16, we performed an ISG15 interactome analysis using anti-ISG15 immunoprecipitation combined with mass spectrometry in HAP1 cells following treatment with type I interferon (IFN-I). USP16 knockout (KO) cells served as controls. Malate dehydrogenase, cytoplasmic (MDH1), superoxide dismutase (SOD) 1, fructose-bisphosphate aldolase A (ALDOA), and cytoplasmic glutamic-oxaloacetic transaminase 1 (GOT1) were identified and confirmed as ISGylated substrates targeted by USP16, suggesting a role for USP16 as a deISGylase in immunometabolic pathways.

Results

Activity-Based Pull-Down Assay Identifies USP16 as an ISG15 Cross-Reactive DUB. To identify ISG15-reactive proteases, we performed pull-down assays with an ISG15 activity-based probe using protein lysates from human HAP1 cells, with or without interferon-α2 (IFN) stimulation. Proteases that reacted with the biotinylated (human) C-terminal domain ISG15 propargylamide (Biotin-hISG15$_{CTD}$-PA) probe (36) were recovered on Streptavidin beads. After washing, elution, and in-solution trypsin digestion, samples were analysed by label-free LC-MS/MS (Fig. 1*A* and Dataset S1). Pull-down efficiency was confirmed by immunoblotting using an anti-biotin antibody prior to analysis by LC-MS/MS (*SI Appendix*, Fig. S1). The LC-MS/MS data were processed by cross-comparative analysis of Biotin-hISG15$_{CTD}$-PA versus "no probe" samples (Fig. 1*B*), and cross-comparative analysis of IFN-stimulated versus control cells (Fig. 1*C*). In the lysates from IFN-stimulated cells, four proteases: USP18, USP14, USP5, and USP16, were significantly enriched in the hISG15$_{CTD}$-PA probe-treated samples (Fig. 1*B*). USP18 was

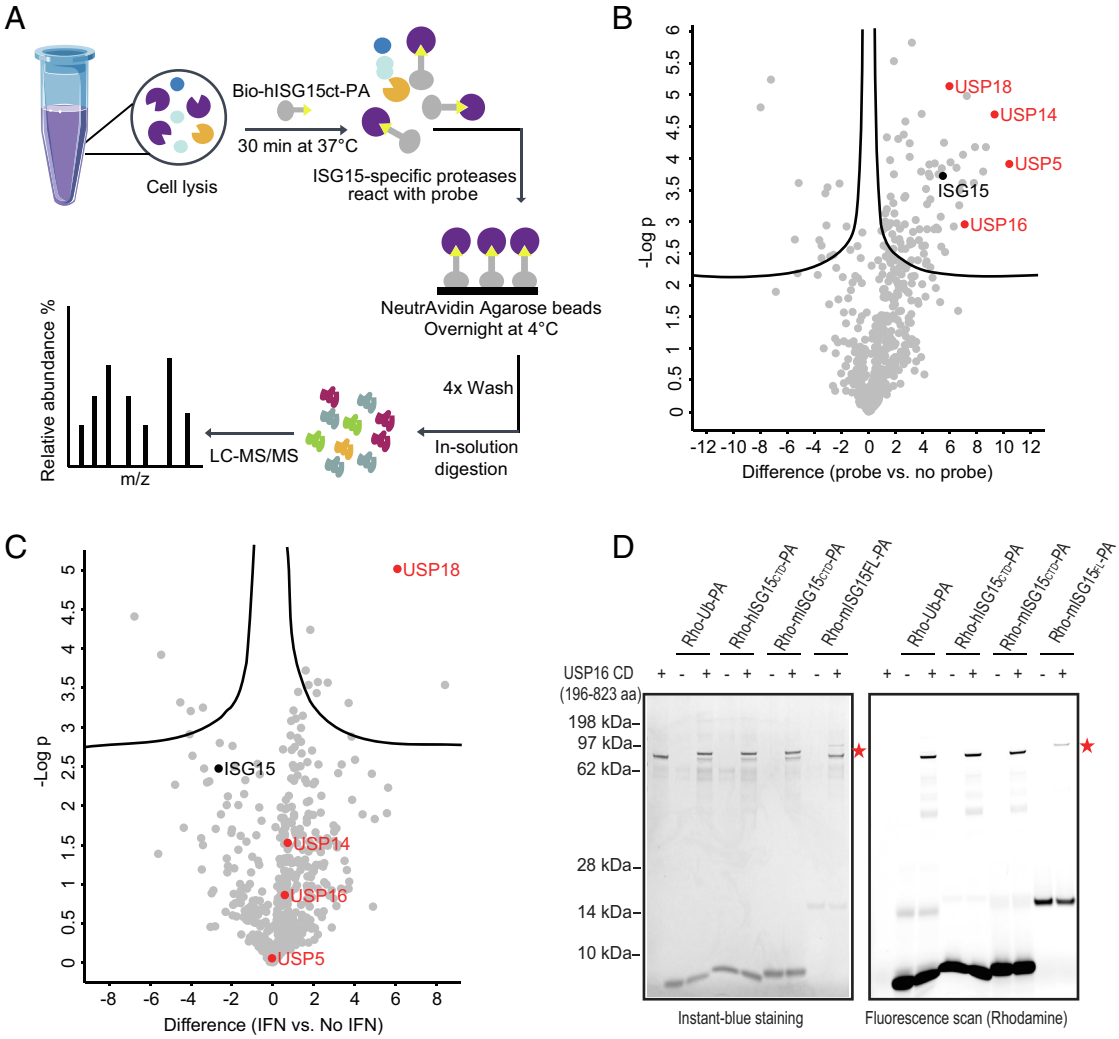

Fig. 1. Activity-based pull-down assay identifies USP16 as an ISG15 cross-reactive DUB (*A*) Streamlined workflow for identification of ISG15-reactive proteases in lysates of HAP1 cells. (*B* and *C*) Volcano plots of a comparative proteomic analysis of the trypsin digests of the materials retrieved by Streptavidin beads. Comparison of biotin-based immunoprecipitation of Biotin-hISG15$_{CTD}$-PA probe labeled versus unlabeled IFN-α2 stimulated HAP1 WT cell lysate (*B*) and comparison of biotin-based immunoprecipitation of IFN-α2 stimulated versus unstimulated cell lysates labeled with Biotin-hISG15$_{CTD}$-PA probe (*C*). The identified Ub/ISG15 proteases are shown in red. The statistical cutoff values used for the proteomic analyses are FDR: 0.01 and s0: 0.1. (*D*) 5 μM of recombinant human USP16 catalytic domain (CD, aa 196-823) reacts with 5 μM of Rhodamine-tagged Ub-PA, as well as human ISG15$_{CTD}$-PA, mouse ISG15$_{CTD}$-PA, and mouse full-length ISG15-PA probes in 10 μL volume at 37 °C for 1 h. After reaction with the probe, samples were denatured, resolved by SDS-PAGE, scanned for fluorescence, and stained with InstantBlue Coomassie dye. The probe-labeled USP16 CD is indicated by red asterisks. Representative data of three (n = 3) independent experiments. See also *SI Appendix*, Fig. S1.

the only hISG15$_{CTD}$-PA-reactive protease that was significantly enriched in the IFN-stimulated cells (Fig. 1*C*).

These data agree with the prior identification of USP18 as an interferon-inducible deISGylase (24, 37). It also corroborates the ability of USP18, USP14, and USP5 to react with a human full-length ISG15 activity-based probe (29–31). Since USP16 was not previously identified as an ISG15-cross-reactive DUB, we verified its ability to bind to both Ub- and ISG15-based probes. Purified recombinant human USP16 was incubated with rhodamine (Rho)-tagged Ub-propargylamide (Rho-Ub-PA) and ISG15-propargylamide (Rho-ISG15-PA) activity-based probes [human ISG15$_{CTD}$-PA (26), mouse ISG15$_{CTD}$-PA (26) and full-length mouse ISG15$_{FL}$-PA (38)], followed by Sodium dodecyl sulfate polyacrylamide gel electrophoresis (SDS-PAGE). Binding to Ub- and ISG15-based probes was confirmed by the presence of the corresponding USP16-probe adducts (Fig. 1*D*).

USP16 Cleaves ISG15-Related Substrates In Vitro. To determine whether USP16 shows catalytic activity toward ISG15, we tested several in vitro substrates that are recognized and converted by deISGylases. We first determined whether USP16 cleaves the 1 to 165 amino acid precursor of human ISG15 (pro-ISG15) (3, 39). We used purified recombinant full-length human USP16 (FL; aa 22-823) and its catalytic domain (CD; aa 196-823). We included deISGylase USP18 and USP5 as positive controls. Recombinant USP7 served as a negative control. The two forms of USP16 cleaved pro-ISG15 as efficiently as recombinant USP18. USP5 was less efficient at cleavage, while USP7 was incapable of cleavage at all (Fig. 2*A*).

We further assessed the isopeptidase activity of USP16 with Ub-based and full-length ISG15-based FP assay substrates. In these substrates, the C-terminal carboxylate of Ub or full-length ISG15 is linked to the lysine ε amine of a fluorescent TAMRA-Lys-Gly peptide, thus mimicking Ub/ISG15 isopeptide-linked substrates (25, 40). We tested purified recombinant USP16FL and USP16CD along with USP18, USP5, and USP7 (Fig. 2*B* and *SI Appendix*, Fig. S2*A*). USP16FL and CD showed cleavage of the ISG15FP substrate at 12.5 nM and completely converted the UbFP substrate at this concentration. USP18 processed the ISG15FP substrate more efficiently than USP16FL or USP16CD. While USP5 and USP7 converted the UbFP substrate at subnanomolar concentrations, they showed no reactivity to the ISG15FP substrate even at 100 nM. USP16 thus has clear isopeptidase activity toward the ISG15FP substrate in vitro.

To determine whether USP16 can remove ISG15 from endogenous ISGylated substrates, we prepared lysates from interferon-β stimulated HAP1 cells deficient for USP18 (USP18KO) (*SI Appendix*, Fig. S2*B*) and incubated these with purified recombinant USP16CD^{WT} or catalytically inactive mutant USP16CD^{C205S}. Wild-type USP16 reduced the amount of ISG15-conjugated proteins in the cell lysate, but as expected, the protease-deficient Cys to Ser mutant did not. We conclude that USP16 deconjugates ISG15 from natural ISGylated substrates through its protease activity (Fig. 2*C*). In conclusion, we show that recombinant USP16 can cleave pro-ISG15 and ISG15FP substrates in vitro and deconjugate endogenous ISGylated proteins in cell lysates.

Loss of USP16 Leads to Increased Cellular ISGylation. Having validated USP16 as an ISG15-cross-reactive DUB, we next examined its deISGylation function in living cells by siRNA-mediated depletion of USP16. Silencing of USP16 in HAP1 cells with three different siRNAs increased ISGylation after stimulation with IFN-β, while the expression level of USP18 remained unchanged (Fig. 3*A*). Next, we used CRISPR/Cas9 to target either exon 6 (KO #A) or exon 4 (KO #B) of USP16 to generate USP16KO HAP1 cell lines. The KO was confirmed by labeling with a USP16-specific Rhodamine-M20-PA probe (41) (*SI Appendix*, Fig. S3*A*) and by immunoblotting (*SI Appendix*, Fig. S3*B*). USP16KO HAP1 cell lines showed increased levels of ISGylation after stimulation with IFN-β (Fig. 3*B*).

The increased ISGylation observed in USP16KO cells could be an indirect effect caused by increased IFN signaling, for instance as a result of reduced USP18-dependent negative feedback by the USP18-IFNAR2-STAT2 inhibitory complex (42). To address this possibility by experiment, we examined whether the USP16KO HAP1 cells showed increased and/or prolonged IFN-induced phosphorylation of the transcription factors STAT1 and STAT2, or enhanced expression of ISGs (43, 44). The levels and kinetics of STAT1 and STAT2 phosphorylation were indistinguishable for USP16KO and WT cells (*SI Appendix*, Fig. S3*C*). Moreover, USP16KO cells did not show changes in interferon-induced ISG15 and USP18 mRNA (*SI Appendix*, Fig. S3*D*), nor altered levels of the interferon-induced proteins RIG-I, MDA5, and USP18 (*SI Appendix*, Fig. S3*E*). The set of deISGlyases detected by the hISG15ct-PA probe was not affected by the USP16KO (*SI Appendix*, Fig. S3*F*). The protein levels and activity of USP16 were unaffected by treatment with IFN-β, in sharp contrast to those of USP18 (*SI Appendix*, Fig. S4 *A* and *B*).

Taken together, a KO of USP16 enhances IFN-β-induced ISGylation and reduces deISGylation without affecting interferon signaling, notwithstanding the presence of USP18. Indeed, the deISGylating activity of USP18, and therefore ISGylation, does not regulate the IFN-I response (45). Furthermore, loss of USP16 cannot be compensated by the activity of USP18. ProISG15 can be efficiently converted to its conjugatable form in the absence of USP16.

Analysis of the USP16-Dependent ISG15 Interactome Connects USP16 to Cellular Metabolism. To obtain global insights in the cellular pathways and functions that may be regulated by the deISGylase activity of USP16, we analysed the ISG15 interactome in HAP1 WT and HAP1 USP16KO cells (both USP16KO clone #A and #B) by immuno-precipitation of ISG15, followed by identification of the retrieved proteins by mass spectrometry (IP-MS) (36). Duplicate dishes were stimulated with IFN-β, with unstimulated cells serving as controls. Cell lysates were subjected to immunoprecipitation with anti-human ISG15 antibody, the immunoprecipitates were digested with trypsin, and the digests subjected to label-free quantitative proteomic analysis (Fig. 4*A* and Dataset S2). The analysis of the ISG15 interactomes, in HAP1 WT cells (*SI Appendix*, Fig. S5*A*) and USP16KO cells (*SI Appendix*, Fig. S5*B*), shows enrichment of the bait (ISG15) and significant enrichment of typical ISGylated proteins, mostly ISGs, upon treatment with IFN-I in agreement with previous studies (46). Comparison of the ISG15 interactomes of USP16KO and WT cells uncovered a USP16-regulated ISG15 interactome of 142 proteins that showed at least a >1.5 fold difference of the Log_2 intensities (USP16KO cells treated with IFN-I versus WT cells treated with IFN-I) (Fig. 4*B* and Dataset S3).

To identify enriched Gene Ontology (GO) terms, we performed PANTHER GO-slim analysis, focusing on cellular compartments (CC), molecular functions (MF), and biological processes (BP) (47–49). The analysis confirmed that the proteins identified as regulated in a USP16-sensitive manner were strongly enriched for enzymes that function in metabolic processes in the cytoplasm and in mitochondria (Fig. 4*C* and *SI Appendix*, Fig. S6). STRING interaction network analysis (50) also showed a large interconnected set of cytoplasmatic and mitochondrial proteins (Fig. 4*D*). Two highly interconnected clusters were identified by the Cytoscape plug-in

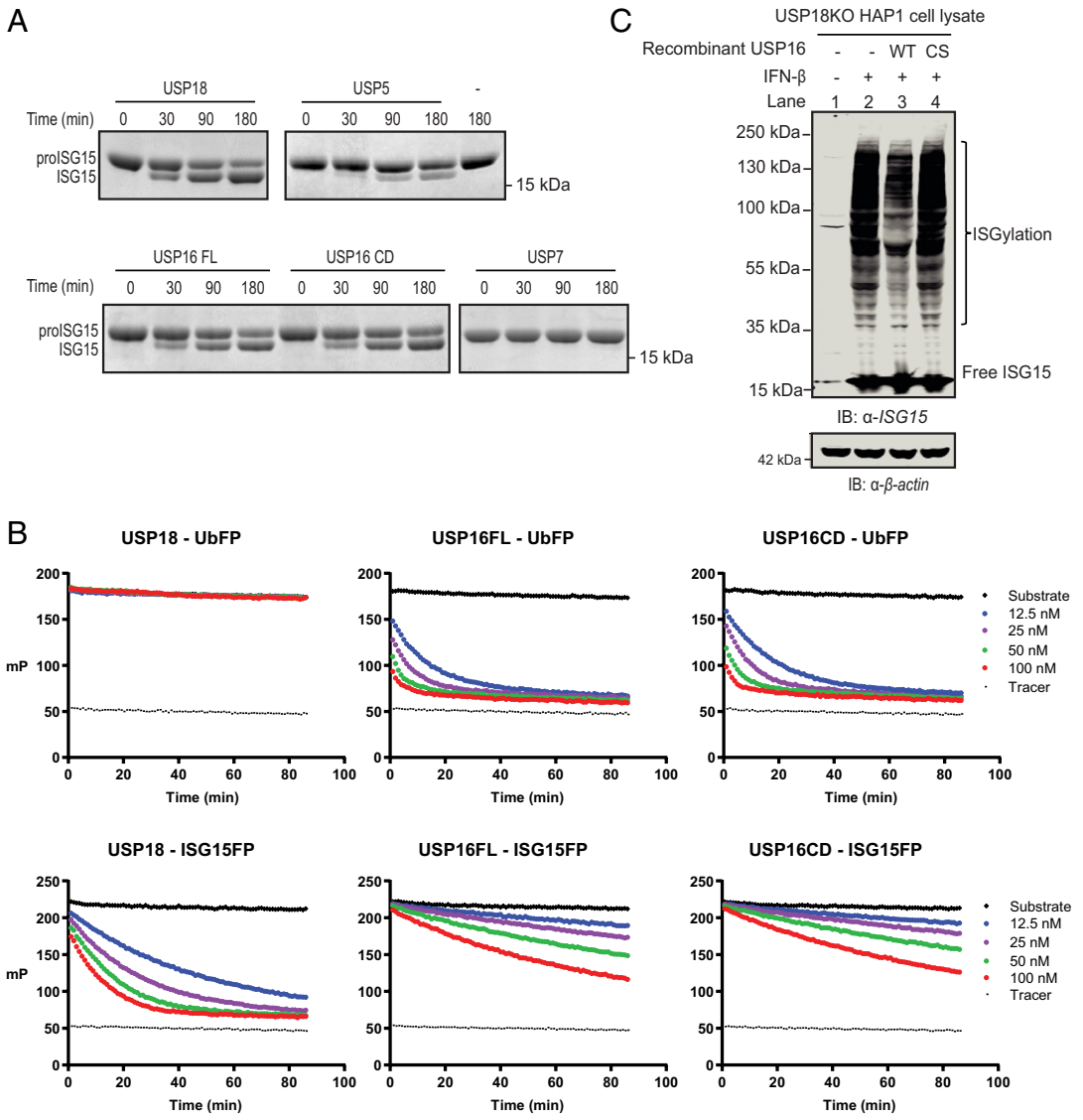

Fig. 2. USP16 cleaves ISG15-related substrates in vitro. (*A*) Human proISG15 is cleaved by recombinant human USP18, USP7, USP5, USP16FL, and USP16CD as analyzed by SDS-PAGE and InstantBlue Coomassie staining. The position of marker proteins is indicated. Representative data of two (n = 2) independent experiments. (*B*) Catalytic activity of recombinant human USP18, USP16FL, and USP16CD toward isopeptide-linked Ub-FP and ISG15-FP substrates. The indicated amounts of USP16 FL/CD were incubated with 200 nM Ub-FP or ISG15-FP. Substrate cleavage was monitored by a change in FP [in millipolarization units (mP)]. Representative data of two (n = 2) independent experiments. (*C*) ISG15 deconjugation in lysates of HAP1 USP18KO cells. HAP1 USP18KO cells were stimulated with IFN-β to induce ISGylation. 40 μg of cell lysate in 10 μL was incubated with recombinant USP16 CD^{WT} or USP16CD^{C205S} at final concentrations of 5 μM at 37 °C for 2 h. Proteins were separated by SDS-PAGE and immunoblotted with anti-human ISG15 antibody. Probing for β-actin served as a loading control. The position of marker proteins is indicated. Representative data of two (n = 2) independent experiments. See also *SI Appendix*, Fig. S2.

MCODE (51), consisting of 15 proteins involved in carbon and pyruvate metabolism, and 9 proteins involved in hydrogen-peroxide metabolic processes (Fig. 4*E*). Importantly, all of these proteins were found to be ISGylated in previous proteomic studies (14, 36, 52–56) (Dataset S4). Collectively, our analysis therefore suggests that the USP16-dependent ISG15 interactome is associated with cellular metabolism.

DeISGylation of Discrete Substrates by USP16. To confirm that selected members of the USP16-sensitive ISG15 interactome are indeed ISGylated and cleaved by USP16, we performed in cellulo ISGylation assays by cotransfection of hUBE1L, UBCH8, HERC5, and Flag-hISG15 in HEK293T cells (14, 57). Ectopic overexpression of USP16 WT, unlike its catalytically inactive mutant $USP16^{C205S}$, decreased overall ISGylation slightly, while overexpression of USP18 WT had stronger effects, as expected (Fig. 5*A*).

Next, we cotransfected Myc-tagged substrates, selected from the two most interconnected clusters identified by the Cytoscape plug-in MCODE analysis (Fig. 4*E*), together with expression constructs for the ISGylation machinery. The latter include hUBE1L, UBCH8, HERC5, and Flag-hISG15. Immunoprecipitation with anti-Myc beads and immunoblotting allowed us to calculate the relative amounts of ISGylated protein. We determined the ratio of the intensity of the ISGylated bands (anti-Flag immunoblot) and the intensity of total protein (anti-Myc immunoblot) and compared these to the normalized amounts of ISGylated protein encoded by the constructs used for transfection. Expression of USP16 WT significantly decreased ISGylation of the metabolic enzymes identified by mass spectrometry (GOT1, ALDOA, SOD1, and MDH1).

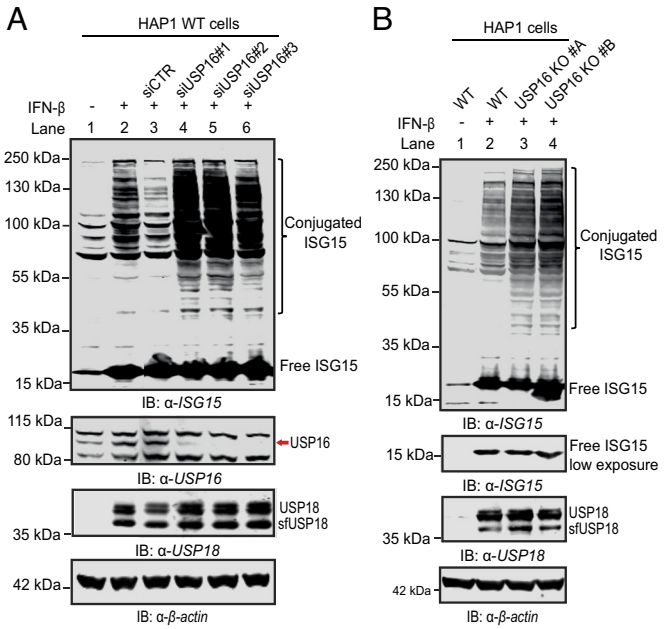

Fig. 3. Loss of USP16 increases cellular ISGylation. (*A*) Knockdown of USP16. HAP1 WT cells were transfected with either control siRNA (siCTR) or three different siRNAs (siUSP16#1, siUSP16#2, and siUSP16#3) against USP16 for 72 h. IFN-β (1,000 U/mL) was added for 24 h prior to harvesting. Lysates were resolved by SDS-PAGE. Immunoblot analysis was performed using the indicated antibodies. (*B*) ISG15 deconjugation in lysates of HAP1 WT and USP16KO cells. Both HAP1 WT and USP16KO cells were stimulated with 1,000 U/mL of IFN-β for 24 h. Cell lysates were resolved by SDS-PAGE and analysed by immunoblotting using the indicated antibodies. For panels *A* and *B*, β-actin served as a loading control. Representative data of three (n = 3) independent experiments. See also *SI Appendix*, Figs. S3 and S4.

Although expression of USP16^{C205S} affected the level of ISGylation to some degree, this effect was never as pronounced as that seen with USP16 WT (Fig. 5 *B*–*E*). In summary, GOT1, ALDOA, SOD1, and MDH1 are ISGylated by the UBE1L-UBCH8-HERC5 cascade in HEK293T cells and are subject to USP16-dependent cleavage.

Discussion

Activity-based probes used to profile Ub and Ub-like processing enzymes have accelerated the discovery of novel members of these families (57–60). Probes generated for different Ubls provided evidence for Ub/Ubl cross-reactivity of several DUBs. For instance, recombinant USP2, USP5, USP13, and USP14 react covalently with an ISG15-vinylsulfone (ISG15-VS) probe (31). This showed that additional cellular deISGylases may exist, in addition to USP18. Also, USP21 has deISGylase activity, as evident from processing of an ISG15-AMC substrate and by in vitro deconjugation of ISGylated proteins from IFN-β stimulated HeLa cells (32). Pull-down experiments performed with immobilized ISG15-propargylamide (ISG15-PA) and ISG15-dehydroalanine (ISG15-Dha) identified the previously reported cross-reactive DUBs USP5, USP14 and USP21 (30, 58). DeISGylase activity for USP5 and USP14 was confirmed using the ISG15-AMC hydrolysis assay. Our study now expands the set of deISGylases by identification of USP16 as an ISG15-cross-reactive DUB in human HAP1 cell lysates. Importantly, we demonstrate activity of USP16 on several ISGylated substrates with potential links to (immuno)metabolism.

Recombinant USP18, USP16, and USP5 can cleave pro-ISG15. Proteolytic processing of the ISG15 precursor protein is required to expose the C-terminal GlyGly motif essential for protein conjugation (3, 39). Since loss of either USP18 or USP16 does not reduce ISGylation (Fig. 3 and *SI Appendix*, Fig. S2*B*), pro-ISG15 processing does not depend on a single enzyme, but is a promiscuous process. ISG15-cross-reactive DUBs, including USP16 and USP5, likely compensate for the loss of USP18 to ensure conversion of pro-ISG15 to ISG15.

We further provide evidence for a deISGylating function of endogenous USP16. We saw enhanced ISGylation in IFN-treated HAP1 cells upon siRNA-mediated silencing and CRISPR/Cas9-mediated deletion of USP16. Interferon signaling itself was not affected by USP16KO or knockdown. Treatment with IFN-β did not alter expression of USP16 or its enzymatic activity as detected by ABPP in HeLa and HAP1 cells, indicating that USP16 is not an interferon-inducible gene. This is in sharp contrast to the main deISGlyase, USP18, and may reflect a different spectrum of activity. Perhaps USP16 deISGylates substrates also in the absence of strong IFN responses, consistent with cell type-dependent basal expression of ISGs (59). The loss of USP16 did not affect type I interferon signaling. Therefore, unlike USP18 (42), USP16 appears not to be implicated in an interferon-based feedback mechanism. Of note, USP18 mediates negative regulation of IFN signaling in a protease-independent manner. This observation also aligns with recent findings that show uncoupling of ISGylation from activation of the IFN-I response pathway (45, 60).

What is the molecular basis for USP16 cross-reactivity? In the absence of a solved structure for USP16, its sequence specifies both a Zinc-finger (ZnF) domain (aa 22-143) and a Ub-specific protease (USP) domain (aa 196-822). The USP domain is responsible for the catalytic activity of USP16, and the ZnF domain has been proposed to recognize glycine at the C-terminal tail of free Ub. This may serve as a sensor for free Ub in cells to regulate Ub-dependent processes (61, 62). Recombinant human USP16 FL (aa 22-823) and CD (aa 196-823) show similar enzymatic activity toward full-length pro-ISG15 and ISG15-FP. The pro-ISG15 processing activity of recombinant human USP16 is thus independent of the ZnF domain. However, the ISG15-based reagents used in this study do not contain the free C-terminal tail of ISG15. It is therefore still unclear whether the ZnF domain of USP16 binds free ISG15 in the same mode as free Ub, and if it plays a regulatory role in ISG15-dependent processes in cells.

The specificity of mouse USP18 for mouse ISG15 is mediated by interaction between a hydrophobic patch in USP18 and a hydrophobic region in the C-terminal domain of ISG15. The C-terminal domain of ISG15 is necessary and sufficient for USP18 binding (26). In our study, the C-terminal domain of human ISG15 was sufficient for reaction with human USP5, USP14, USP16, and USP18. This domain must therefore determine ISG15 cross-reactivity of DUBs. Human USP18 reacts with mouse ISG15-PA (26). Likewise, recombinant human USP16 displayed cross-species reactivity toward the mouse ISG15-PA probe (Fig. 1*D*). While this work was under review, it was shown that recombinant USP16 cleaves ISG15(CTD)-KG-TAMRA model substrates (63), corroborating our findings in Fig. 2*B*. USP16 was also shown to recognize Fubi (63, 64). A high-resolution structure of USP16 in complex with Ub, Fubi, and ISG15, not available as of today, could establish the molecular basis for these interactions.

USP16 was initially identified as a DUB that removes Ub from lysine119 of H2A (33, 65). Many other ubiquitinated substrates for USP16 have been identified so far (66). The USP16-dependent ISG15 interactome identified in our experiments contained mostly cytoplasmic proteins, suggesting that USP16 exerts its function there. None of the reported substrates of USP16-mediated

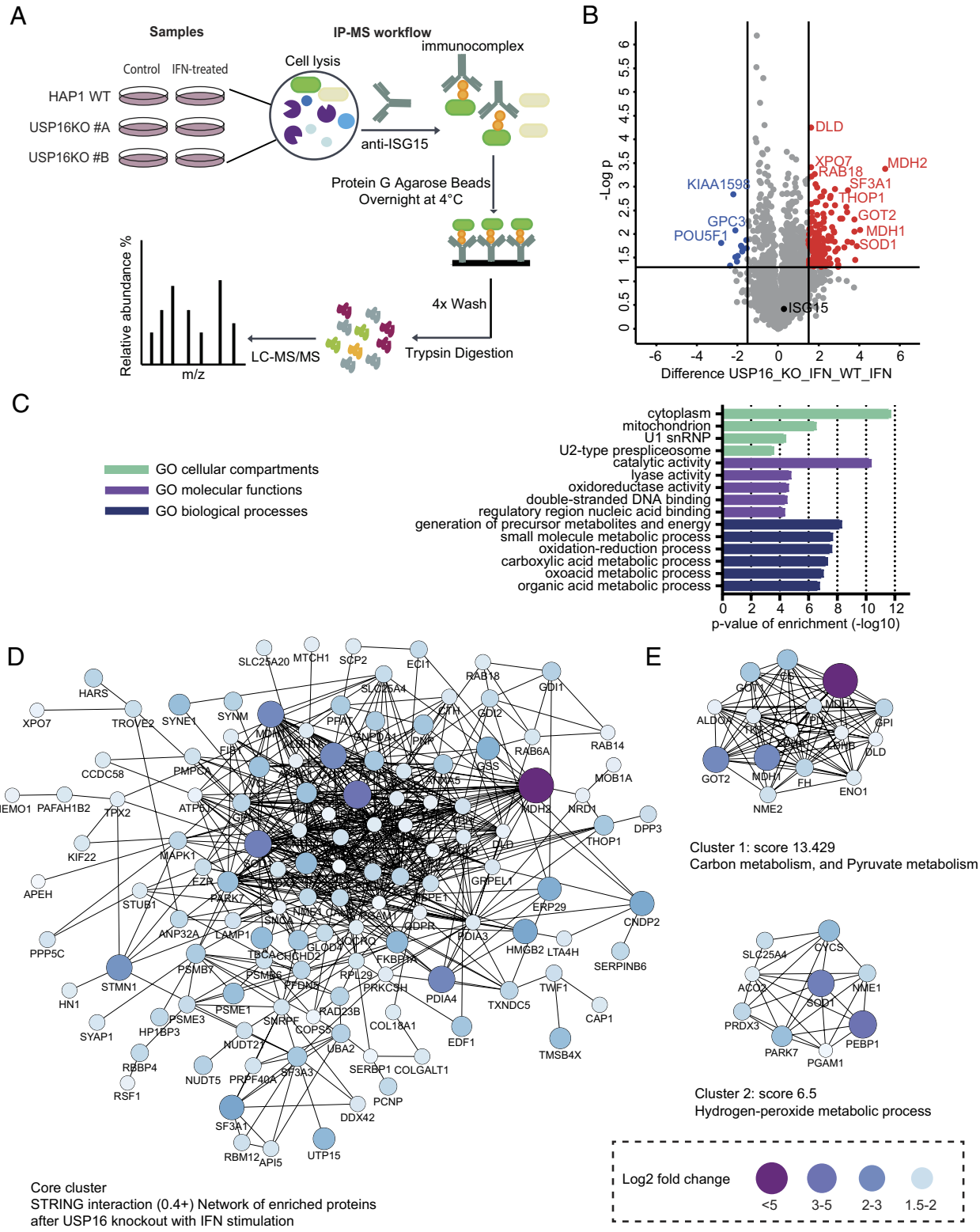

Fig. 4. Analysis of the USP16-dependent ISG15 interactome links USP16 to cellular metabolism. (*A*) Schematic representation of the workflow for ISG15 immunoprecipitation mass spectrometry (IP-MS) used to analyze the ISG15 interactome. HAP1 WT and USP16KO cells were stimulated by 1,000 U/mL of IFN-β for 48 h to produce ISGylated substrates (two biological replicates). (*B*) Volcano plot showing all proteins identified for the IFN-β stimulated USP16KO samples, compared to the IFN-β stimulated WT HAP1 cells. Dashed lines indicate a cutoff at a difference of the Log2 intensities bigger than 1.5 and a *P* value of 0.05 (−log10 = 1.3), n = 2 independent experiments. Proteins in red showed increased interaction with ISG15 in the USP16KO cells compared to the WT cells. These are termed the "USP16-dependent ISG15 interactome". Proteins indicated in blue showed decreased levels in the USP16KO cells compared to WT cells. (*C*) GO enrichment analysis of the USP16-dependent ISG15 interactome. The bar graph shows the most significantly overrepresented GO terms for CC in light green, MF in purple, and BP in dark blue, compared against the annotated human proteome. The full GO terms for MF are found in *SI Appendix*, Fig. S7*A* and BP are found in *SI Appendix*, Fig. S7*B*. (*D*) STRING network analysis of the USP16-dependent ISG15 interactome, with a STRING interaction confidence of 0.4 or higher. Cytoscape software was used to visualize the interaction network. Color and node size indicate the differences (of the Log2-transformed intensities) in abundance for USP16KO HAP1 cells compared with the WT HAP1 control upon IFN-β treatment. (*E*) Cluster 1 and cluster 2 contain multiple proteins involved in carbon and pyruvate metabolism and hydrogen peroxide metabolic process, respectively. MCODE was used to extract the most highly interconnected clusters (clusters 1 and 2) from the network shown in (*D*). See also *SI Appendix*, Figs. S5 and S6.

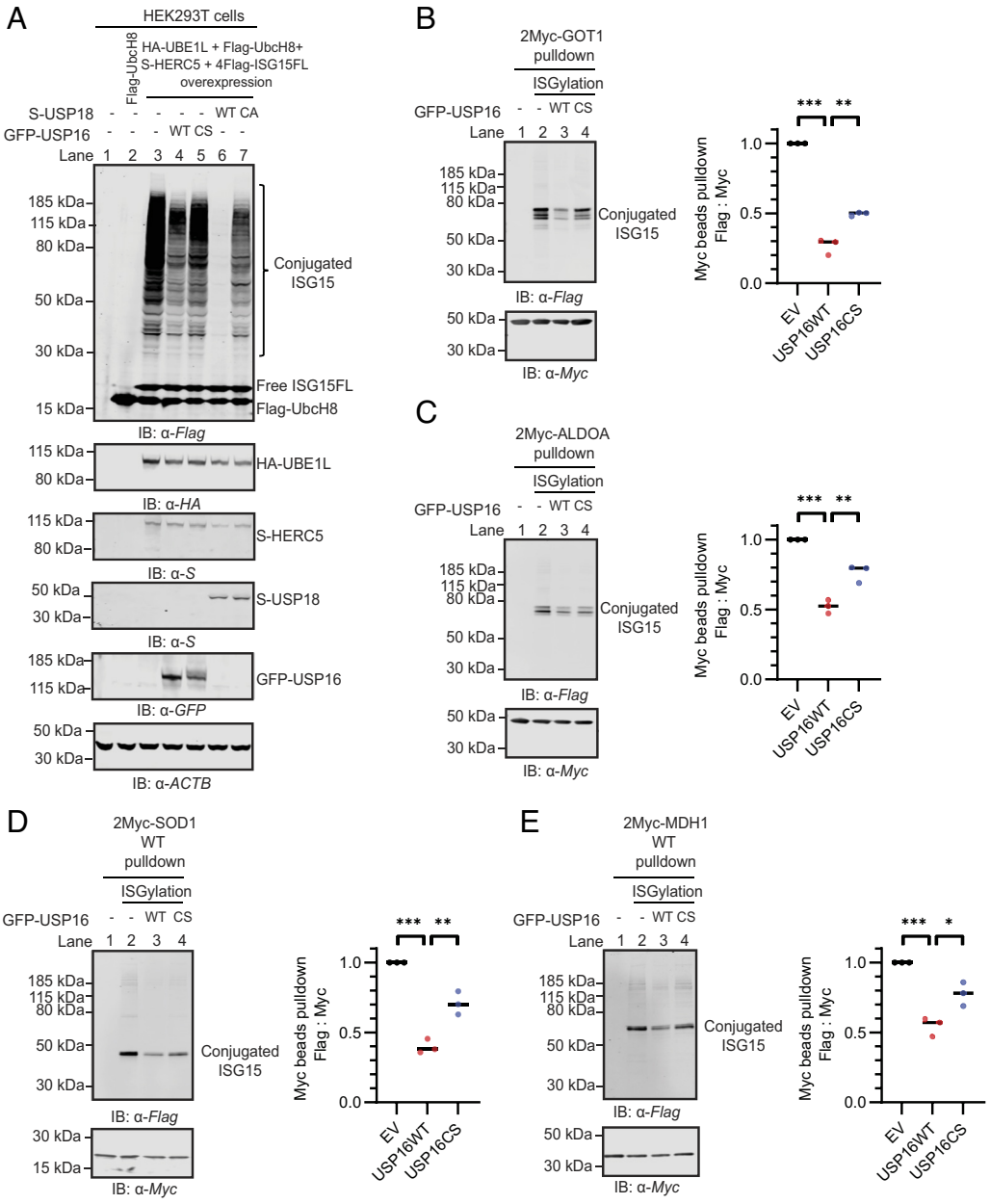

Fig. 5. Validation of selected proteins as ISGylated substrates for deISGylation by USP16. (*A*) DeISGylation assay in HEK293T cells that overexpress USP16 or USP18. Cellular ISGylation was achieved by cotransfecting an ISGylation plasmid mixture including 2 μg HA-UBE1L, 2 μg Flag-UBCH8, 2 μg S-HERC5, and 2 μg Flag ISG15 in HEK293T cells in 6-cm dishes for 24 h. Empty vector (4 μg; lane 3), USP16 WT/C205S, or USP18 WT/C64A were cotransfected with plasmids encoding the ISGylation machinery as indicated. Cell lysates were resolved by SDS-PAGE and analysed by immunoblotting using the indicated antibodies. Representative data of three (n = 3) independent experiments. (*B–E*) Validation of $(Myc)_2$-GOT1 (*B*), $(Myc)_2$-ALDOA1 (*C*), $(Myc)_2$-SOD1 (*D*), and $(Myc)_2$-GOT1 (*E*) as ISGylated substrates for USP16-mediated deISGylation by staining the immunoblot with anti-Flag antibodies to detect Flag-ISG15. Plasmids encoding $(Myc)_2$-tagged substrates protein were cotransfected with plasmids encoding ISGylation machinery, and GFP empty vector (EV), GFP-USP16WT or GFP-USP16C205S mutant in HEK293T cells in 6 cm dishes for 24 h. $(Myc)_2$-tagged proteins were immunoprecipitated from the cell lysates by Myc trap beads. The retrieved proteins were interrogated by immunoblot using the indicated antibodies. Quantification of the amounts of ISGylated protein in lanes 2 to 4 by detection with the anti-Myc and anti-Flag antibodies. The ratio of anti-flag vs. anti-Myc protein intensity was normalized to the EV control. Bar graphs report mean; error bars reflect ± SD of three (n = 3) independent experiments. All *P* values were calculated using Student's *t* test: $^{**}P < 0.05$, $^{***}P < 0.001$, and NS = not significant.

deubiquitination were found in the USP16-dependent ISG15 interactome from IFN-β-stimulated HAP1 cells.

ISGylation is a key element of the innate immune response by modification of host or viral proteins, in order to restrict the replication or spread of pathogens (67). However, ISGylation has also been linked to mitochondrial functions and cellular metabolism (68, 69), which may also be important for innate immunity. The enrichment of the USP16-dependent ISG15 interactome for metabolic enzymes that function in the cytoplasm and in mitochondria is consistent with a role for ISG15 in the regulation of cellular metabolism and mitochondrial function. This characteristic of the USP16-dependent ISG15-interactome is quite distinct from the previously studied USP18-dependent ISG15 interactome, in which primarily proteins involved in interferon signaling, innate immune responses, and virus defense responses are enriched (36). ISGylated metabolic enzymes GOT1, ALDOA, SOD1 and MDH1 were confirmed as bona fide targets of USP16 deISGylase activity (Fig. 6). Three of the enzymes are involved in gluconeogenesis (GOT1, MDH1, and ALDOA). The consequences of their USP16-dependent deISGylation may affect immunometabolism in general and cellular gluconeogenesis in

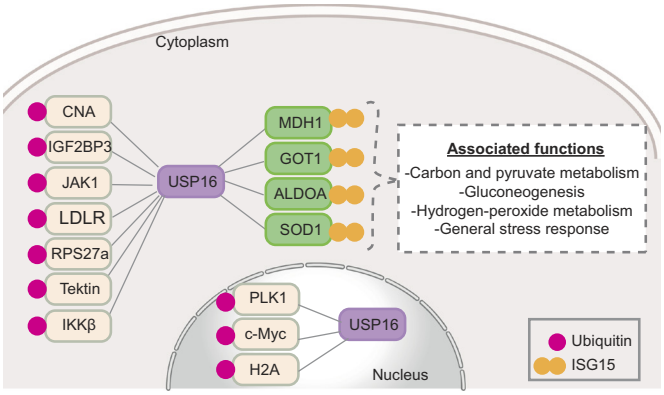

Fig. 6. Overview of the roles of USP16 as a dual deubiquitylating and deISGylating enzyme. Canonical ubiquitylated protein substrates are colored in yellow and novel ISGylated metabolic enzyme substrates in green.

particular. Antagonists of USP16 could be important tool compounds to study immunometabolism.

Materials and Methods

ABPP with the Biotin-ISG15-PA Probe. ABPP was performed as previously described (70). HAP1 cells were lysed using glass beads in lysis buffer (GBL: 50 mM Tris, pH 7.5, 5 mM $MgCl_2$, 0.5 mM EDTA, and 250 mM Sucrose). Protein concentrations were determined using the Pierce BCA Assay. One milligram of protein was labelled with Biotin-ISG15-PA at the predetermined optimum ratio and incubated for 30 min (Viva Biotech Ltd) at 37 °C. The reaction was quenched by addition of 5% (w/v) SDS and 10% NP-40 to each sample. Samples were then diluted by adding NP-40 lysis buffer, and NeutrAvidin Agarose beads (Thermo Fisher) were added prior incubation for 16 h at 4 °C (with rotation). The beads were washed with NP-40 Lysis four times in total. Probe-labelled proteins were eluted from the beads by addition of LSLB with 3 mM biotin and boiled (10 min, 95 °C). Eluted materials were subjected to immunoblotting and LC/MS/MS analysis (70).

Immunoprecipitation to Recover the ISG15 Interactome. Immunoprecipitations were performed as described (36) with the following modifications. HAP1 cells were lysed with lysis buffer (20 mM Hepes pH 8.0, 150 mM NaCl, 0.2% NP-40, 10% glycerol, 5 mM NEM, phosphatase, and protease inhibitor cocktails; 25×10^6 cells per condition) and subjected to immunoprecipitation using 5 μg of anti-ISG15 antibody (Boston Biochem #A-380) and 25 μL of protein G Sepharose slurry (Invitrogen; #15920-10) for 16 h at 4 °C. Beads were washed 4 times with lysis buffer. Immune complexes were eluted with 2X Laemmli sample buffer. One-tenth of the eluates was used for immunoblotting with the indicated antibodies. The remaining eluate was prepared for analysis by MS as previously described (71) using suspension traps (S-Traps). Proteins were reduced with 200 mM DTT in 0.1 M Tris pH 7.8, followed by alkylation with 200 mM iodoacetamide in 0.1 M Tris pH 7.8 in the dark. Samples were acidified by addition of 12% phosphoric acid and captured on S-TrapTM midi columns (C02-midi, ProtiFi). Columns were washed with 90% methanol in 100 mM triethylammonium bicarbonate by centrifugation at 4,000 g. Captured proteins were digested with trypsin (1:100 w/w) overnight at room temperature. Peptides were dried and dissolved in Buffer A (98% MilliQ-H_2O, 2% CH_3CN, and 0.1% TFA).

Additional descriptions of the methods are listed in *SI Appendix, SI Methods*.

Data, Materials, and Software Availability. All study data are included in the article and/or supporting information. The mass spectrometry proteomics data have been deposited to the ProteomeXchange Consortium via the PRIDE partner repository with the dataset identifier PXD043553 (72).

ACKNOWLEDGMENTS. This work was supported by the Oncode Institute, The Netherlands Organization for Scientific Research (VICI grant no. 724.013.002 to H.O.), and the Institute for Chemical Immunology (grant no. ICI00026 to A.S.). The A.P.-F. and B.M.K. labs were supported by the Chinese Academy of Medical Sciences Innovation Fund for Medical Science, China (grant number: 2018-I2M-2-002) and by Pfizer. Work in the lab of H.L.P. is supported by a Director's Pioneer award (DP1AI150593) from the NIH. This study also received funding from the Deutsche Forschungsgemeinschaft (DFG, German Research Foundation) under Germany's Excellence Strategy (CIBSS–EXC-2189–Project ID 390939984) and DFG Project-ID 259373024 – TRR 167.

Author affiliations: [a]Department of Cell and Chemical Biology, Division of Chemical Biology and Drug Discovery, Leiden University Medical Center, Leiden 2333 ZC, The Netherlands; [b]Program in Cellular and Molecular Medicine, Boston Children's Hospital, Harvard Medical School, Boston, MA 02115; [c]Chinese Academy for Medical Sciences Oxford Institute, Nuffield Department of Medicine, University of Oxford, Oxford OX3 7BN, United Kingdom; [d]Target Discovery Institute, Nuffield Department of Medicine, Centre for Medicines Discovery, University of Oxford, Oxford OX3 7FZ, United Kingdom; [e]Department of Cell and Chemical Biology and Oncode Institute, Leiden University Medical Center LUMC, Leiden 2333 ZC, The Netherlands; [f]Department of Cellular Microbiology, University of Hohenheim, Stuttgart 70599, Germany; [g]Institute of Neuropathology, Faculty of Medicine, Department of Molecular Genetics, University of Freiburg, Freiburg 79106, Germany; and [h]Centre for Integrative Biological Signalling Studies, Department of Molecular Genetics, University of Freiburg, Freiburg 79104, Germany

Author contributions: J.G., A.P.-F., H.O., B.M.K., P.P.G., and A.S. designed research; J.G., A.P.-F., D.F., J.J.L.L.A., D.P.O., H.G., H.C.S., and P.P.G. performed research; A.P.-F., G.F., K.-P.K., and B.M.K. contributed new reagents/analytic tools; J.G., A.P.-F., H.L.P., B.M.K., and A.S. analyzed data; J.N. provided supervison; and J.G., A.P.-F., J.N., H.v.D., H.L.P., P.P.G., and A.S. wrote the paper.

1. A. L. Haas, P. Ahrens, P. Bright, H. Ankel, Interferon induces a 15-kilodalton protein exhibiting marked homology to ubiquitin. *J. Biol. Chem.* **262**, 11315–11323 (1987).
2. D. Zhang, D. E. Zhang, Interferon-stimulated gene 15 and the protein ISGylation system. *J. Interferon Cytokine Res.* **31**, 119–130 (2011).
3. J. L. Potter, J. Narasimhan, L. Mende-Mueller, A. L. Haas, Precursor processing of pro-ISG15/UCRP, an interferon-beta-induced ubiquitin-like protein. *J. Biol. Chem.* **274**, 25061–25068 (1999).
4. E. Knight Jr., B. Cordova, IFN-induced 15-kDa protein is released from human lymphocytes and monocytes. *J. Immunol.* **146**, 2280–2284 (1991).
5. M. Recht, E. C. Borden, E. Knight Jr., A human 15-kDa IFN-induced protein induces the secretion of IFN-gamma. *J. Immunol.* **147**, 2617–2623 (1991).
6. D. Bogunovic *et al.*, Mycobacterial disease and impaired IFN-γ immunity in humans with inherited ISG15 deficiency. *Science* **337**, 1684–1688 (2012).
7. P. F. Dos Santos, D. S. Mansur, Beyond ISGlylation: Functions of free intracellular and extracellular ISG15. *J. Interferon Cytokine Res.* **37**, 246–253 (2017).
8. O. A. Malakhova, D. E. Zhang, ISG15 inhibits Nedd4 ubiquitin E3 activity and enhances the innate antiviral response. *J. Biol. Chem.* **283**, 8783–8787 (2008).
9. Y. H. Yeh, Y. C. Yang, M. Y. Hsieh, Y. C. Yeh, T. K. Li, A negative feedback of the HIF-1α pathway via interferon-stimulated gene 15 and ISGylation. *Clin. Cancer Res.* **19**, 5927–5939 (2013).
10. X. Zhang *et al.*, Human intracellular ISG15 prevents interferon-alpha/beta over-amplification and auto-inflammation. *Nature* **517**, 89–93 (2015).
11. W. Yuan, R. M. Krug, Influenza B virus NS1 protein inhibits conjugation of the interferon (IFN)-induced ubiquitin-like ISG15 protein. *EMBO J.* **20**, 362–371 (2001).
12. C. Zhao *et al.*, The UbcH8 ubiquitin E2 enzyme is also the E2 enzyme for ISG15, an IFN-alpha/beta-induced ubiquitin-like protein. *Proc. Natl. Acad. Sci. U.S.A.* **101**, 7578–7582 (2004).
13. K. I. Kim, N. V. Giannakopoulos, H. W. Virgin, D. E. Zhang, Interferon-inducible ubiquitin E2, Ubc8, is a conjugating enzyme for protein ISGylation. *Mol. Cell. Biol.* **24**, 9592–9600 (2004).
14. J. J. Wong, Y. F. Pung, N. S. Sze, K. C. Chin, HERC5 is an IFN-induced HECT-type E3 protein ligase that mediates type I IFN-induced ISGylation of protein targets. *Proc. Natl. Acad. Sci. U.S.A.* **103**, 10735–10740 (2006).
15. W. Zou, D. E. Zhang, The interferon-inducible ubiquitin-protein isopeptide ligase (E3) EFP also functions as an ISG15 E3 ligase. *J. Biol. Chem.* **281**, 3989–3994 (2006).
16. F. Okumura, W. Zou, D.-E. Zhang, ISG15 modification of the eIF4E cognate 4EHP enhances cap structure-binding activity of 4EHP. *Genes Dev.* **21**, 255–260 (2007).
17. L. Ketscher, A. Basters, M. Prinz, K. P. Knobeloch, mHERC6 is the essential ISG15 E3 ligase in the murine system. *Biochem. Biophys. Res. Commun.* **417**, 135–140 (2012).
18. D. Oudshoorn *et al.*, HERC6 is the main E3 ligase for global ISG15 conjugation in mouse cells. *PLoS One* **7**, e29870 (2012).
19. S. D. Desai *et al.*, Elevated expression of ISG15 in tumor cells interferes with the ubiquitin/26S proteasome pathway. *Cancer Res.* **66**, 921–928 (2006).
20. J. B. Fan *et al.*, Identification and characterization of a novel ISG15-ubiquitin mixed chain and its role in regulating protein homeostasis. *Sci. Rep.* **5**, 12704 (2015).
21. M. Liu, X. L. Li, B. A. Hassel, Proteasomes modulate conjugation to the ubiquitin-like protein, ISG15. *J. Biol. Chem.* **278**, 1594–1602 (2003).
22. Y. J. Jeon *et al.*, ISG15 modification of filamin B negatively regulates the type I interferon-induced JNK signalling pathway. *EMBO Rep.* **10**, 374–380 (2009).
23. Z. Kuang, E. J. Seo, J. Leis, Mechanism of inhibition of retrovirus release from cells by interferon-induced gene ISG15. *J. Virol.* **85**, 7153–7161 (2011).
24. M. P. Malakhov, O. A. Malakhova, K. I. Kim, K. J. Ritchie, D. E. Zhang, UBP43 (USP18) specifically removes ISG15 from conjugated proteins. *J. Biol. Chem.* **277**, 9976–9981 (2002).
25. A. Basters *et al.*, Molecular characterization of ubiquitin-specific protease 18 reveals substrate specificity for interferon-stimulated gene 15. *FEBS J.* **281**, 1918–1928 (2014).
26. A. Basters *et al.*, Structural basis of the specificity of USP18 toward ISG15. *Nat. Struct. Mol. Biol.* **24**, 270–278 (2017).

27. K. J. Ritchie *et al.*, Role of ISG15 protease UBP43 (USP18) in innate immunity to viral infection. *Nat. Med.* **10**, 1374–1378 (2004).
28. L. Ketscher *et al.*, Selective inactivation of USP18 isopeptidase activity in vivo enhances ISG15 conjugation and viral resistance. *Proc. Natl. Acad. Sci. U.S.A.* **112**, 1577–1582 (2015).
29. T. Wang *et al.*, Expedient synthesis of ubiquitin-like protein ISG15 tools through chemo-enzymatic ligation catalyzed by a viral protease Lb(pro). *Angew. Chem. Int. Ed. Engl.* **61**, e202206205 (2022).
30. C. Li *et al.*, Simultaneous capture of ISG15 conjugating and deconjugating enzymes using a semi-synthetic ISG15-Dha probe. *Sci. China Chem.* **66**, 837–844 (2023).
31. A. Catic *et al.*, Screen for ISG15-crossreactive deubiquitinases. *PLoS One* **2**, e679 (2007).
32. Y. Ye *et al.*, Polyubiquitin binding and cross-reactivity in the USP domain deubiquitinase USP21. *EMBO Rep.* **12**, 350–357 (2011).
33. H. Y. Joo *et al.*, Regulation of cell cycle progression and gene expression by H2A deubiquitination. *Nature* **449**, 1068–1072 (2007).
34. C. Montellese *et al.*, USP16 counteracts mono-ubiquitination of RPS27a and promotes maturation of the 40S ribosomal subunit. *Elife* **9**, e54435 (2020).
35. J.-S. Yu *et al.*, Substrate-specific recognition of IKKs mediated by USP16 facilitates autoimmune inflammation. *Sci. Adv.* **7**, eabc4009 (2021).
36. A. Pinto-Fernandez *et al.*, Deletion of the deISGylating enzyme USP18 enhances tumour cell antigenicity and radiosensitivity. *Br J. Cancer* **124**, 817–830 (2021), 10.1038/s41416-020-01167-y.
37. D.-C. Kang, H. Jiang, Q. Wu, S. Pestka, P. B. Fisher, Cloning and characterization of human ubiquitin-processing protease-43 from terminally differentiated human melanoma cells using a rapid subtraction hybridization protocol RaSH. *Gene* **267**, 233–242 (2001).
38. B. T. Xin *et al.*, Total chemical synthesis of murine ISG15 and an activity-based probe with physiological binding properties. *Org. Biomol. Chem.* **17**, 10148–10152 (2019).
39. E. Knight *et al.*, A 15-kDa interferon-induced protein is derived by COOH-terminal processing of a 17-kDa precursor. *J. Biol. Chem.* **263**, 4520–4522 (1988).
40. P. P. Geurink, F. El Oualid, A. Jonker, D. S. Hameed, H. Ovaa, A general chemical ligation approach towards isopeptide-linked ubiquitin and ubiquitin-like assay reagents. *Chembiochem* **13**, 293–297 (2012).
41. L. Gjonaj *et al.*, Development of a DUB-selective fluorogenic substrate. *Chem. Sci.* **10**, 10290–10296 (2019).
42. K. I. Arimoto *et al.*, STAT2 is an essential adaptor in USP18-mediated suppression of type I interferon signaling. *Nat. Struct. Mol. Biol.* **24**, 279–289 (2017).
43. K. I. Kim *et al.*, Enhanced antibacterial potential in UBP43-deficient mice against Salmonella typhimurium infection by up-regulating type I IFN signaling. *J. Immunol.* **175**, 847–854 (2005).
44. W. Zou *et al.*, Microarray analysis reveals that Type I interferon strongly increases the expression of immune-response related genes in Ubp43 (Usp18) deficient macrophages. *Biochem. Biophys. Res. Commun.* **356**, 193–199 (2007).
45. V. Jové *et al.*, Human USP18 protects diverse cancer lineages from Type I Interferon independently of its canonical catalytic function. bioRxiv [Preprint] (2023). https://doi.org/10.1101/2023.03.23.533924 (Accessed 16 November 2023).
46. F. Thery, D. Eggermont, F. Impens, Proteomics mapping of the ISGylation landscape in innate immunity. *Front. Immunol.* **12**, 720765 (2021).
47. Gene Ontology Consortium, The Gene Ontology resource: Enriching a GOld mine. *Nucleic acids Res.* **49**, D325–D334 (2021).
48. M. Ashburner *et al.*, Gene ontology: Tool for the unification of biology. The Gene Ontology Consortium. *Nat. Genet.* **25**, 25–29 (2000).
49. H. Mi, A. Muruganujan, D. Ebert, X. Huang, P. D. Thomas, PANTHER version 14: More genomes, a new PANTHER GO-slim and improvements in enrichment analysis tools. *Nucleic Acids Res.* **47**, D419–D426 (2019).
50. D. Szklarczyk *et al.*, The STRING database in 2021: Customizable protein-protein networks, and functional characterization of user-uploaded gene/measurement sets. *Nucleic Acids Res.* **49**, D605–D612 (2021).
51. G. D. Bader, C. W. V. Hogue, An automated method for finding molecular complexes in large protein interaction networks. *BMC Bioinformatics* **4**, 1–27 (2003).
52. S. Yan *et al.*, IRF3 reduces adipose thermogenesis via ISG15-mediated reprogramming of glycolysis. *J. Clin. Invest.* **131**, e144888 (2021).
53. N. V. Giannakopoulos *et al.*, Proteomic identification of proteins conjugated to ISG15 in mouse and human cells. *Biochem. Biophys. Res. Commun.* **336**, 496–506 (2005).
54. T. Takeuchi, S. Inoue, H. Yokosawa, Identification and Herc5-mediated ISGylation of novel target proteins. *Biochem. Biophys. Res. Commun.* **348**, 473–477 (2006).
55. Y. Zhang *et al.*, The in vivo ISGylome links ISG15 to metabolic pathways and autophagy upon Listeria monocytogenes infection. *Nat. Commun.* **10**, 5383 (2019).
56. C. Zhao, C. Denison, J. M. Huibregtse, S. Gygi, R. M. Krug, Human ISG15 conjugation targets both IFN-induced and constitutively expressed proteins functioning in diverse cellular pathways. *Proc. Natl. Acad. Sci. U.S.A.* **102**, 10200–10205 (2005).
57. L. A. Durfee, J. M. Huibregtse, Identification and validation of ISG15 target proteins. *Subcell Biochem.* **54**, 228–237 (2010).
58. T. Wang *et al.*, Expedient synthesis of ubiquitin-like protein ISG15 tools through chemo-enzymatic ligation catalyzed by a viral protease Lb^{pro}. *Angew. Chem. Int. Ed. Engl.* **61**, e202206205 (2022), 10.1002/anie.202206205.
59. H. Liu *et al.*, Tumor-derived IFN triggers chronic pathway agonism and sensitivity to ADAR loss. *Nat. Med.* **25**, 95–102 (2019).
60. A. Clancy *et al.*, ISGylation-independent protection of cell growth by USP18 following interferon stimulation. *Biochem J.* **480**, 1571–1581 (2023).
61. M. T. Pai *et al.*, Solution structure of the Ubp-M BUZ domain, a highly specific protein module that recognizes the C-terminal tail of free ubiquitin. *J. Mol. Biol.* **370**, 290–302 (2007).
62. J. Bonnet, C. Romier, L. Tora, D. Devys, Zinc-finger UBPs: Regulators of deubiquitylation. *Trends Biochem. Sci.* **33**, 369–375 (2008).
63. Z. Zhao, R. O'Dea, K. Wendrich, N. Kazi, M. Gersch, Native semisynthesis of isopeptide-linked substrates for specificity analysis of deubiquitinases and Ubl proteases. *J. Am. Chem. Soc.* **145**, 20801–20812 (2023).
64. R. O'Dea *et al.*, Molecular basis for ubiquitin/fubi cross-reactivity in USP16 and USP36. *Nat. Chem. Biol.* **19**, 1394–1405 (2023), 10.1038/s41589-023-01388-1.
65. M. Adorno *et al.*, Usp16 contributes to somatic stem-cell defects in Down's syndrome. *Nature* **501**, 380–384 (2013).
66. J. Zheng *et al.*, The pleiotropic ubiquitin-specific peptidase 16 and its many substrates. *Cells* **12**, 886 (2023).
67. Y. C. Perng, D. J. Lenschow, ISG15 in antiviral immunity and beyond. *Nat. Rev. Microbiol.* **16**, 423–439 (2018).
68. S. Baldanta *et al.*, ISG15 governs mitochondrial function in macrophages following vaccinia virus infection. *PLoS Pathog.* **13**, e1006651 (2017).
69. S. Alcalá *et al.*, ISG15 and ISGylation is required for pancreatic cancer stem cell mitophagy and metabolic plasticity. *Nat. Commun.* **11**, 2682 (2020).
70. A. Pinto-Fernández *et al.*, Comprehensive landscape of active deubiquitinating enzymes profiled by advanced chemoproteomics. *Front. Chem.* **7**, 592 (2019).
71. L. Dietz *et al.*, Structural basis for SMAC-mediated antagonism of caspase inhibition by the giant ubiquitin ligase BIRC6. *Science* **379**, 1112–1117 (2023).
72. J. Gan *et al.*, Proteomics data in "USP16 is an ISG15 cross-reactive deubiquitinase targeting a subset of metabolic pathway-related proteins". Proteomics Identification Database. https://www.ebi.ac.uk/pride/archive/projects/PXD043553. Deposited 17 November 2023.